

# Renal Transporter-Mediated Drug-Biomarker Interactions of the Endogenous Substrates Creatinine and N<sup>1</sup>-Methylnicotinamide: A PBPK Modeling Approach

Denise Türk<sup>1</sup> , Fabian Müller<sup>2</sup>, Martin F. Fromm<sup>2</sup> , Dominik Selzer<sup>1</sup>, Robert Dallmann<sup>3</sup>  and Thorsten Lehr<sup>1,\*</sup> 

Endogenous biomarkers for transporter-mediated drug-drug interaction (DDI) predictions represent a promising approach to facilitate and improve conventional DDI investigations in clinical studies. This approach requires high sensitivity and specificity of biomarkers for the targets of interest (e.g., transport proteins), as well as rigorous characterization of their kinetics, which can be accomplished utilizing physiologically-based pharmacokinetic (PBPK) modeling. Therefore, the objective of this study was to develop PBPK models of the endogenous organic cation transporter (OCT)2 and multidrug and toxin extrusion protein (MATE)1 substrates creatinine and N<sup>1</sup>-methylnicotinamide (NMN). Additionally, this study aimed to predict kinetic changes of the biomarkers during administration of the OCT2 and MATE1 perpetrator drugs trimethoprim, pyrimethamine, and cimetidine. Whole-body PBPK models of creatinine and NMN were developed utilizing studies investigating creatinine or NMN exogenous administration and endogenous synthesis. The newly developed models accurately describe and predict observed plasma concentration-time profiles and urinary excretion of both biomarkers. Subsequently, models were coupled to the previously built and evaluated perpetrator models of trimethoprim, pyrimethamine, and cimetidine for interaction predictions. Increased creatinine plasma concentrations and decreased urinary excretion during the drug-biomarker interactions with trimethoprim, pyrimethamine, and cimetidine were well-described. An additional inhibition of NMN synthesis by trimethoprim and pyrimethamine was hypothesized, improving NMN plasma and urine interaction predictions. To summarize, whole-body PBPK models of creatinine and NMN were built and evaluated to better assess creatinine and NMN kinetics while uncovering knowledge gaps for future research. The models can support investigations of renal transporter-mediated DDIs during drug development.

## Study Highlights

### WHAT IS THE CURRENT KNOWLEDGE ON THE TOPIC?

☑ Investigations on renal transporter-mediated drug-drug interactions (DDIs) are impeded due to challenging *in vitro* to *in vivo* translation.

### WHAT QUESTION DID THIS STUDY ADDRESS?

☑ How can the application of a biomarker-informed approach support conventional investigation on DDIs and how can mechanistic mathematical modeling contribute to assess biomarker kinetics?

### WHAT DOES THIS STUDY ADD TO OUR KNOWLEDGE?

☑ The endogenous biomarkers creatinine and N<sup>1</sup>-methylnicotinamide have been proposed as biomarkers to

support investigations on renal transporter-mediated DDIs. Whole-body physiologically-based pharmacokinetic models have been developed and successfully applied for interaction predictions with three established renal transporter inhibitors.

### HOW MIGHT THIS CHANGE CLINICAL PHARMACOLOGY OR TRANSLATIONAL SCIENCE?

☑ Mechanistic pharmacokinetic modeling has been shown to support characterization of endogenous compounds and a biomarker-informed strategy for investigations on interactions might be a promising approach during drug development.

<sup>1</sup>Clinical Pharmacy, Saarland University, Saarbrücken, Germany; <sup>2</sup>Institute of Experimental and Clinical Pharmacology and Toxicology, Friedrich-Alexander-Universität Erlangen-Nürnberg, Erlangen, Germany; <sup>3</sup>Division of Biomedical Sciences, Warwick Medical School, University of Warwick, Coventry, UK. \*Correspondence: Thorsten Lehr ([thorsten.lehr@mx.uni-saarland.de](mailto:thorsten.lehr@mx.uni-saarland.de))

Received March 11, 2022; accepted April 28, 2022. doi:10.1002/cpt.2636

Endogenous compounds measured in blood or urine can serve as biomarkers, providing information about physiological and pharmacological processes. Pathophysiological conditions or interaction of a perpetrator drug with the synthesis, distribution, metabolism, or excretion of a biomarker can result in changes of plasma, tissue, or urine levels. Measuring biomarkers can complement investigations on drug-drug interactions (DDIs) by broadening and augmenting the understanding of underlying interaction mechanisms, thus, estimating DDI risks in early-stage *in vivo* studies and supporting study planning and prioritization.<sup>1</sup> Mathialagan *et al.*<sup>2</sup> pointed out challenges of *in vitro-in vivo* translation for renal transporter-mediated DDIs and emphasized the need for a biomarker-informed strategy to improve DDI risk predictions from *in vitro* data. For the renal organic cation secretion axis, represented by consecutive action of organic cation transporter (OCT)2 and multidrug and toxin extrusion proteins (MATEs),<sup>3</sup> two endogenous compounds have been identified as potential biomarkers to investigate interactions: creatinine and N<sup>1</sup>-methylnicotinamide (NMN).<sup>4</sup> Creatinine, a breakdown product of muscle creatine, is mainly excreted passively via glomerular filtration, but 10–40% are actively secreted,<sup>5</sup> mainly by OCT2 and MATEs,<sup>6</sup> whereas no metabolism of creatinine has been described previously. NMN, a molecule formed during tryptophan and vitamin B3 metabolism, is metabolized via aldehyde oxidase (AOX)<sup>7</sup> and passively renally cleared as well as actively transported into urine by OCT2 and MATEs.<sup>8,9</sup> NMN renal clearance is concentration-dependent comparing intravenous administration to endogenously synthesized NMN, attributed to saturable reabsorption from urine.<sup>10</sup>

When identifying and selecting a biomarker for interaction studies, various factors need to be considered, such as sensitivity, specificity, predictivity, robustness, and ease of accessibility.<sup>11,12</sup> Furthermore, biomarkers need to be well-characterized regarding their kinetics, including their endogenous synthesis, active transport, and metabolic transformation. However, detailed information on these processes is often lacking (e.g., due to the complex interplay of transport and metabolism as well as requirements for dedicated studies and analytical procedures<sup>12,13</sup>). Here, physiologically-based pharmacokinetic (PBPK) modeling can help to support investigations on endogenous compounds and to gain a mechanistic understanding of the underlying kinetics.<sup>12</sup> Over the past years, PBPK modeling has become an increasingly important tool during drug development,<sup>14</sup> and has shown its strengths and advantages (e.g., in accurately describing and predicting (pharmacokinetics) of victims during perpetrator co-administration<sup>15</sup> or in assessing the influence of genetic polymorphisms<sup>16</sup>). Furthermore, PBPK models have proven their capability for hypothesis testing (e.g., regarding causes for altered renal transport of drugs in patients with chronic kidney disease<sup>17</sup>). For endogenous biomarkers, there are examples of successfully utilizing PBPK models, to assess and understand transporter-mediated interactions using coproporphyrin I or creatinine.<sup>18–23</sup> However, there is still an apparent lack of PBPK models for endogenous compounds to overcome,<sup>12</sup> in particular for renal OCT2/MATE substrates.

Biomarker PBPK models can support investigations on transporter-mediated DDIs. A PBPK model for an investigational

drug (and potential OCT2 and/or MATE inhibitor) can be linked with biomarker PBPK models in early clinical phases during drug development, to assess the interaction potential. For instance, inhibitory constant ( $K_i$ ) values from *in vitro* tests can be implemented and model predictions can be compared with biomarker plasma and clearance measurements from phase I studies, to complement the workflow for utilization of endogenous biomarkers in drug development, as proposed by Mathialagan *et al.*<sup>2</sup> This includes assessing the influence of a new drug on biomarker renal clearance before performing a metformin DDI study, if *in vitro* inhibition studies hint toward OCT2 and/or MATE inhibition potential.

The objectives of this study were (1) to develop whole-body PBPK models of the endogenous biomarkers creatinine and NMN that mechanistically describe their absorption, synthesis, metabolic transformation, and active transport also considering causes of observed diurnal variation, and (2) to test the ability of the newly developed models to adequately describe drug-biomarker interactions (DBIs) with the potent OCT2 and MATE inhibitors trimethoprim, pyrimethamine, and cimetidine,<sup>24</sup> by coupling the biomarker models to already evaluated and published perpetrator models within a PBPK DDI/DBI modeling network.<sup>17,25,26</sup>

## METHODS

### Software

PBPK models of creatinine and NMN were developed using the PK-Sim and MoBi modeling software suite (Open Systems Pharmacology Suite 9.1, [www.open-systems-pharmacology.org](http://www.open-systems-pharmacology.org)). Plasma and urine measurements from literature were digitized with Engauge Digitizer 10.12 (M. Mitchell<sup>27</sup>) according to best practices.<sup>28</sup> Model parameter optimization and sensitivity analysis were performed within MoBi. Calculation of (pharmacokinetic) parameters, quantitative model performance analysis, and generation of plots were accomplished using the statistical programming language R 4.1.1 (The R Foundation for Statistical Computing, Vienna, Austria) and RStudio 1.4.1717 (RStudio, Boston, MA).

### PBPK model building

An extensive literature search was performed to gather physicochemical information about creatinine and NMN as well as information about important kinetic processes, such as absorption, synthesis, distribution, metabolism, and excretion (compound-dependent parameters). Additionally, studies reporting human blood and urine measurements after intravenous and oral administration in single- and multiple-dose regimens were collected alongside concentration measurements of endogenous creatinine and NMN. For creatinine, studies investigating its kinetics after ingestion of cooked meat were also included by calculating creatinine intake from the amount of ingested meat considering the animal source and method of preparation (e.g., 1.5 mg creatinine per gram of boiled beef<sup>29</sup>). Profiles extracted from clinical studies were digitized and subsequently divided into a training dataset for model building and a test dataset for model evaluation. Data for model building were selected to include plasma and urine measurements after exogenous administration of different doses and regimens of creatinine or NMN (corrected for endogenous levels) as well as endogenous concentrations. Virtual twins of (mean) study subjects were created with demographic information taken from the respective study reports. Detailed information about virtual individuals and system-dependent parameters is provided in **Supplementary Section S1.1**. Endogenous synthesis of creatinine and NMN was implemented in the respective organs in agreement with literature reports. Diurnal variation of kidney-related processes has been recently observed to affect the pharmacokinetics of the renal transporter

substrate metformin (D. Türk *et al.*, unpublished data) and was therefore implemented for both creatinine and NMN (**Supplementary Section S1.1**). Creatinine and NMN model parameters which could not be based on published values, were optimized by fitting training simulations to their respective observed data. Details on parameter optimizations are provided in **Supplementary Section S1.1**.

### PBPK model evaluation

Creatinine and NMN model performances were evaluated by comparison of predicted to observed plasma concentration-time and urine profiles as well as by goodness-of-fit plots. Quantitative model performance was evaluated by calculating mean relative deviations of predicted plasma concentrations and urinary excretion rates ( $Ae_{urine}$  rates) as well as geometric mean fold errors (GMFEs) of predicted area under the concentration-time curve calculated from the time of compound administration (or first data sampling point) to the time of the last concentration measurement ( $AUC_{last}$ ) and maximum plasma concentration ( $C_{max}$ ) values, amounts excreted unchanged in urine ( $Ae_{urine}$ ) and renal clearances, as described elsewhere.<sup>17,25</sup> Local sensitivity analyses were performed for the creatinine and NMN models to investigate the impact of single parameter changes on predicted  $AUC_{last}$  values.

### Drug-biomarker interaction modeling

Models of trimethoprim,<sup>25</sup> pyrimethamine,<sup>26</sup> and cimetidine<sup>17</sup> have been recently or, in the case of pyrimethamine, during this analysis (**Supplementary Section S5**), successfully applied to predict DDIs with the OCT1, OCT2, and MATE substrate metformin using interaction parameters from the literature. Hence, these models were considered eligible for interaction predictions with the newly developed creatinine and NMN models. Model parameters are reproduced in **Tables S18, S21, S28, and S32**.

DBI model performances were evaluated by comparison of predicted to observed plasma concentration-time or urine profiles before and during, or without and with perpetrator drug administration, depending on the

respective observed dataset. Furthermore, comparison of predicted to observed DBI  $AUC_{last}$ ,  $C_{max}$ , and urinary excretion ratios, calculated as ratio of the respective DBI kinetic parameter to the respective control kinetic parameter, was displayed in goodness-of-fit plots and GMFEs were calculated as quantitative measures.

## RESULTS

### Creatinine PBPK model building and evaluation

A total of 26 studies were included to develop a whole-body creatinine PBPK model, covering creatinine kinetics of endogenous creatinine as well as kinetics after intravenous and oral administration and after dietary meat consumption. All clinical studies used for model building and evaluation are listed in **Table S2**.

The final creatinine PBPK model covers its synthesis in muscle cells (individually optimized for each study, range synthesis rate ( $R_{syn}$ ) 6.50–11.88  $\mu\text{mol}/\text{min}$ ; **Table S5**) based on endogenously synthesized creatinine. Creatinine is mainly excreted passively via glomerular filtration, but to a lower extent actively secreted by sequential action of OCT2 and MATE1. Tubular secretion accounts for about 17% of renal clearance in the model. This is in accordance with the literature, which reports a contribution of tubular secretion by 10–40% to renal creatinine clearance ( $CL_{cr}$ ).<sup>5</sup> An increase in serum creatinine by meat ingestion has been shown by several studies, being most pronounced for cooked beef.<sup>30</sup> For instance, ingestion of 225 g cooked beef corresponds to about 340 mg creatinine<sup>29</sup> and leads to a transient increase in plasma creatinine by 40%,<sup>31</sup> which was reproduced by the model. Observed intraday variation of creatinine plasma concentrations was described by diurnal renal excretion comprising diurnal glomerular filtration rate (GFR), renal blood flow, and OCT2

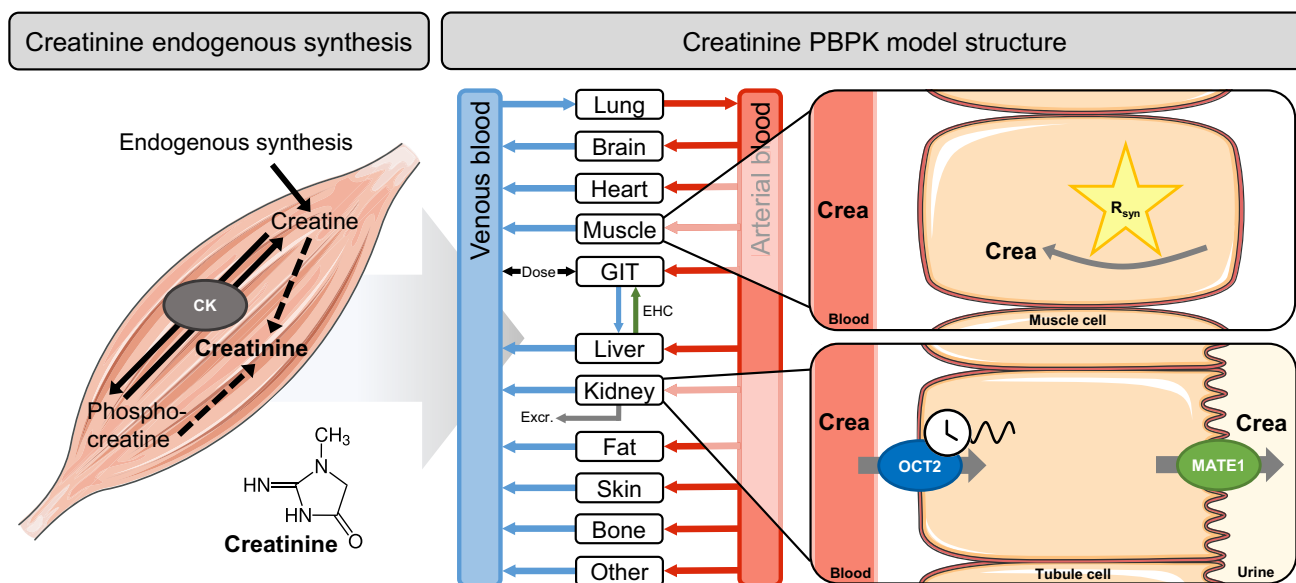


**Figure 1** Synthesis of endogenous creatinine and whole-body physiologically-based pharmacokinetic (PBPK) model processes. Creatinine is formed as breakdown product during reaction of creatine to phosphocreatine and vice versa via creatine kinase (CK). The creatinine PBPK model includes creatinine synthesis in muscle cells (implemented as  $R_{syn}$ , synthesis rate) and renal excretion, passively via glomerular filtration (not shown) and actively via consecutive action of organic cation transporter (OCT)2 and multidrug and toxin extrusion protein (MATE)1 in tubule epithelial cells. Diurnal rhythm is implemented for glomerular filtration rate (GFR), renal blood flow (both not shown) and OCT2 activity (clock symbol). Drawings by Servier, licensed under CC BY 3.0.<sup>44</sup> Crea, creatinine; EHC, enterohepatic circulation; excr., excretion; GIT, gastrointestinal tract. [Colour figure can be viewed at [wileyonlinelibrary.com](http://wileyonlinelibrary.com)]

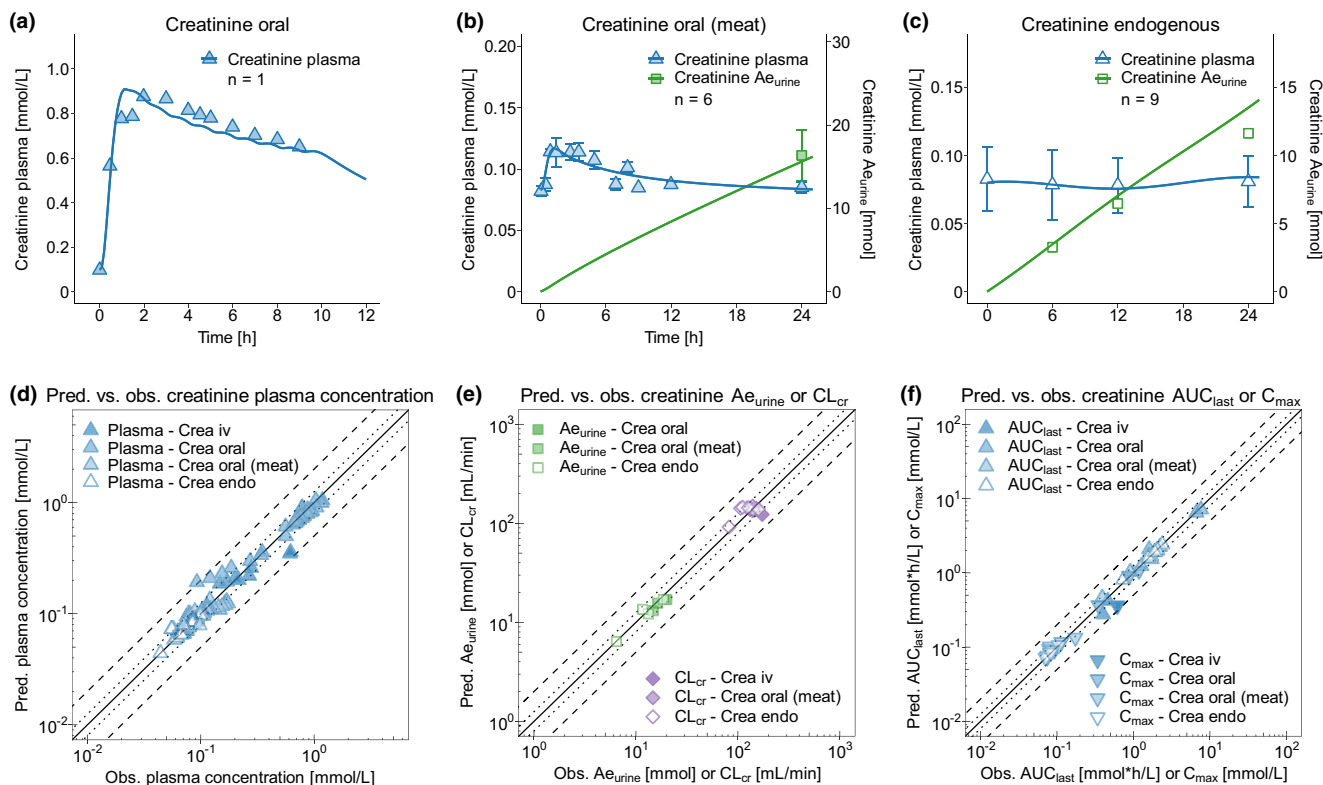


**Figure 2** Creatinine physiologically-based pharmacokinetic (PBPK) model performance. Predictions of creatinine (a–c) plasma concentration–time (blue) and cumulative amount excreted unchanged in urine ( $Ae_{urine}$ , green) profiles compared with observed data of representative studies<sup>31,45,46</sup> of exogenous creatinine application **a** initial oral dose of 8 g creatinine followed by 0.5 g every hour; **b** ingestion of 225 g cooked beef, or **c** endogenous measurements. Time refers to the time after dose (exogenous) or time after first concentration measurement (endogenous). Goodness-of-fit plots showing predicted compared with observed creatinine (d) plasma concentration, (e)  $Ae_{urine}$ , and renal creatinine clearance ( $CL_{cr}$ ) and (f) area under the concentration–time curve ( $AUC_{last}$ ) and maximum plasma concentration ( $C_{max}$ ) values of all studies used for model building and evaluation. The solid line marks the line of identity and dotted lines indicate 1.25-fold and dashed lines indicate 2-fold deviation. Data are shown as blue triangles (plasma), green squares ( $Ae_{urine}$ ), and purple diamonds ( $CL_{cr}$ ); filled symbols indicate creatinine administration, empty symbols indicate endogenous creatinine. Details on the clinical studies and individual values alongside mean relative deviations (MRDs) and geometric mean fold errors (GMFEs) are provided in **Supplementary Section S2**. Crea, creatinine; endo, endogenous; iv, intravenous; n, number of individuals studied; obs., observed; pred., predicted. [Colour figure can be viewed at [wileyonlinelibrary.com](https://onlinelibrary.wiley.com/doi/10.1002/cpt.2636)]

activity. An overview of the creatinine synthesis, model structure, and implemented kinetic processes is illustrated in **Figure 1**. Creatinine compound-dependent model parameters are summarized in **Table S3**.

Representative creatinine plasma concentration–time and  $Ae_{urine}$  profiles are shown in **Figure 2a–c**, demonstrating the good performance of the creatinine model. Profiles of all studies are provided in **Supplementary Section S2.2**. Comparison of predicted to observed creatinine plasma concentration,  $Ae_{urine}$ ,  $CL_{cr}$ ,  $AUC_{last}$ , and  $C_{max}$  values in goodness-of-fit plots further underlines the good performance of the creatinine model with all predictions within twofold of observed values (**Figure 2d–f**). A local sensitivity analysis revealed that simulations of creatinine are sensitive to the fraction unbound in plasma (literature value), GFR (calculated), and creatinine  $R_{syn}$  (optimized).

### NMN PBPK model building and evaluation

A total of 11 studies was used to develop a whole-body NMN PBPK model, covering NMN kinetics after intravenous administration and endogenous NMN. All clinical studies used for model building and evaluation are listed in **Table S10**.

The final NMN PBPK model covers synthesis in liver cells (individually optimized for each study; **Table S13**), metabolism via AOX1 as well as glomerular filtration and active transport into urine by OCT2 and MATE1. Furthermore, a saturable tubular re-absorption process has been implemented as efflux transport at the basolateral site of tubule cells, whereas Michaelis-Menten and transport rate constants were inferred from high (intravenous administration) and low (baseline) NMN plasma levels and the corresponding urinary excretion rates. For an intravenous administration of 224 mg NMN, the model predicts a metabolized fraction of about 40% compared with 33% reported in literature.<sup>32</sup> Regarding endogenously synthesized NMN, renal clearance accounts for 18–36% of total clearance (depending on the daytime), which is in accordance with the observed data, where 35% of NMN and its carboxamide metabolites in urine are unchanged NMN.<sup>7</sup> Observed intraday variation of NMN plasma concentrations was described by a combination of diurnal NMN synthesis and renal excretion comprising diurnal GFR, renal blood flow, and OCT2 activity, using a modified equation<sup>33</sup> for NMN  $R_{syn}$  (**Supplementary Section S1.1**). An overview of the NMN synthesis, model structure, and implemented kinetic processes is



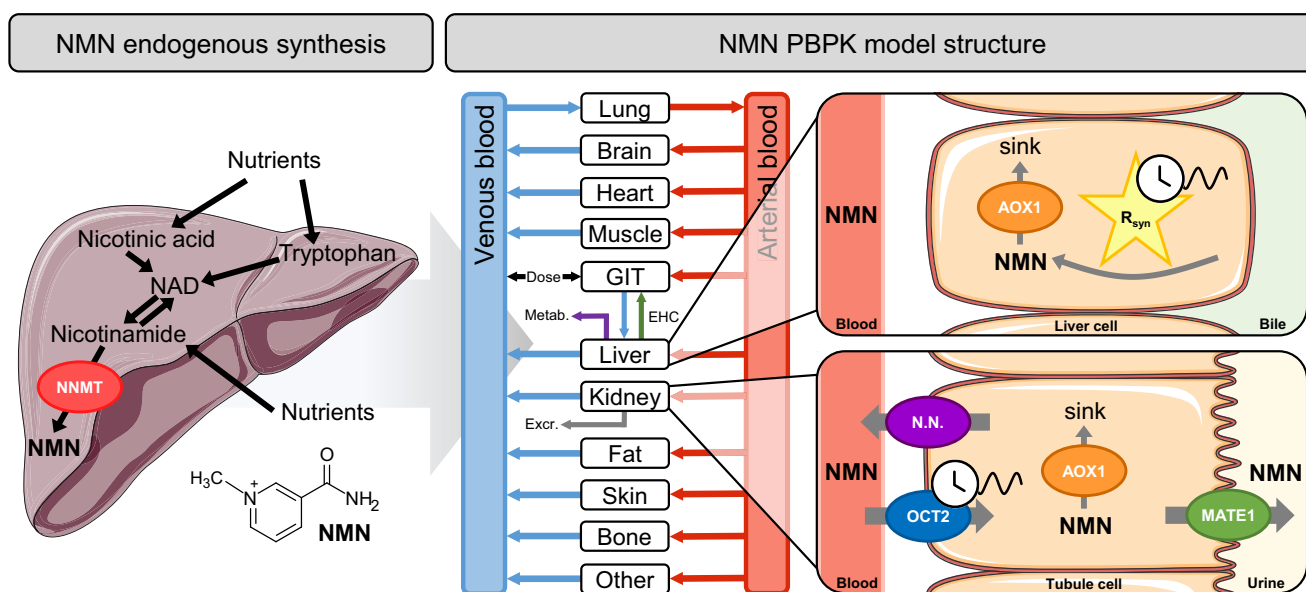


**Figure 3** Synthesis of endogenous  $N^1$ -methylnicotinamide (NMN) and whole-body physiologically-based pharmacokinetic (PBPK) model processes. NMN is synthesized from nutrients via various intermediates. The direct precursor nicotinamide is converted to NMN via nicotinamide N-methyltransferase (NNMT), which is mainly expressed in liver cells.<sup>47</sup> The NMN PBPK model covers NMN synthesis in the liver (implemented as  $R_{syn}$ , synthesis rate) and metabolism by aldehyde oxidase (AOX)1, where resulting carboxamide metabolites are not included in the model (“sink” process). NMN is passively excreted in urine via glomerular filtration (not shown), actively secreted via organic cation transporter (OCT)2 and multidrug and toxin extrusion protein (MATE)1 and re-absorbed from urine via a saturable process (“N.N.”), implemented at the basolateral site of tubule cells. Diurnal rhythm is implemented for glomerular filtration rate (GFR), renal blood flow (both not shown), OCT2 activity, and NMN  $R_{syn}$  (clock symbols). Drawings by Servier, licensed under CC BY 3.0.<sup>44</sup> EHC, enterohepatic circulation; excr., excretion; GIT, gastrointestinal tract; metab., metabolism, NAD, nicotinamide adenine dinucleotide. [Colour figure can be viewed at [wileyonlinelibrary.com](https://onlinelibrary.wiley.com/doi/10.1002/cpt.2636)]

illustrated in **Figure 3**. NMN compound-dependent model parameters are summarized in **Table S11**.

Representative NMN plasma concentration-time,  $Ae_{urine}$  rate and  $Ae_{urine}$  profiles are shown in **Figure 4a–c**, demonstrating the good performance of the NMN model. Profiles of all studies are provided in **Supplementary Section S3.2**. Comparison of predicted to observed NMN plasma concentration,  $Ae_{urine}$  rate and  $Ae_{urine}$  and  $AUC_{last}$  and  $C_{max}$  values in goodness-of-fit plots further underlines the good performance of the NMN model with about 90% of predictions within twofold of observed values (**Figure 4d–f**). A local sensitivity analysis revealed that both simulations of intravenously administered and endogenous NMN are sensitive to the fraction unbound in plasma (literature value) and simulations of endogenous NMN are sensitive to OCT2 activity (optimized), AOX1 clearance (optimized), and organ permeability (calculated).

### Drug-biomarker interaction modeling

A renal transporter DBI network was established (**Figure 5**) by linking the biomarker models with models of trimethoprim, pyrimethamine, and cimetidine. Specifically, OCT2 competitive inhibition was modeled with literature  $K_i$  values of 47.8  $\mu\text{mol/L}$ , 0.61  $\mu\text{mol/L}$ , and 124  $\mu\text{mol/L}$ , and MATE1 competitive inhibition was modeled with literature  $K_i$  values of 4.45  $\mu\text{mol/L}$ , 0.02  $\mu\text{mol/L}$ , and 3.80  $\mu\text{mol/L}$  for trimethoprim, pyrimethamine, and cimetidine, respectively (**Tables S18, S21, S32**). For all perpetrators, the same inhibition constants were used as for previous interaction predictions with metformin.

To evaluate the drug-creatinine interactions, eight, three and two studies with trimethoprim, pyrimethamine, and cimetidine, respectively, have been utilized and are listed in **Tables S34, S37, and S40**. During administration of trimethoprim, pyrimethamine, and cimetidine, an increase in serum creatinine and a decrease of creatinine  $Ae_{urine}$  and  $CL_{cr}$  has been observed. This kinetic interaction can be attributed to inhibition of tubular secretion of creatinine. Observed plasma concentration-time and urine profiles are well-described, indicating a good drug-creatinine interaction model performance. Representative predicted creatinine profiles before and during trimethoprim or cimetidine and without and with pyrimethamine compared with observed data are shown in **Figure 6**. Plots of all profiles are provided in **Supplementary Section S7**.

Predicted DBI  $AUC_{last}$ ,  $C_{max}$ ,  $Ae_{urine}$ , and  $CL_{cr}$  ratios are all within twofold of observed ratios and within prediction limits proposed by Guest *et al.*<sup>34</sup> (**Figure 6**). Corresponding values for all clinical studies are provided in **Tables S35, S36, S38, S39, and S41**, including calculated overall GMFEs.

To model the drug-NMN interactions, one trimethoprim and two pyrimethamine studies were incorporated and are listed in **Tables S42 and S46**. During administration of trimethoprim and pyrimethamine, a decrease of NMN  $Ae_{urine}$  has been observed, resulting from inhibition of NMN transport by OCT2 and MATE1, which the model was able to (partially) reproduce. Conversely, NMN plasma concentration time profiles during trimethoprim and pyrimethamine interaction result in lower mean NMN concentrations compared with control profiles<sup>8,9,35</sup> and

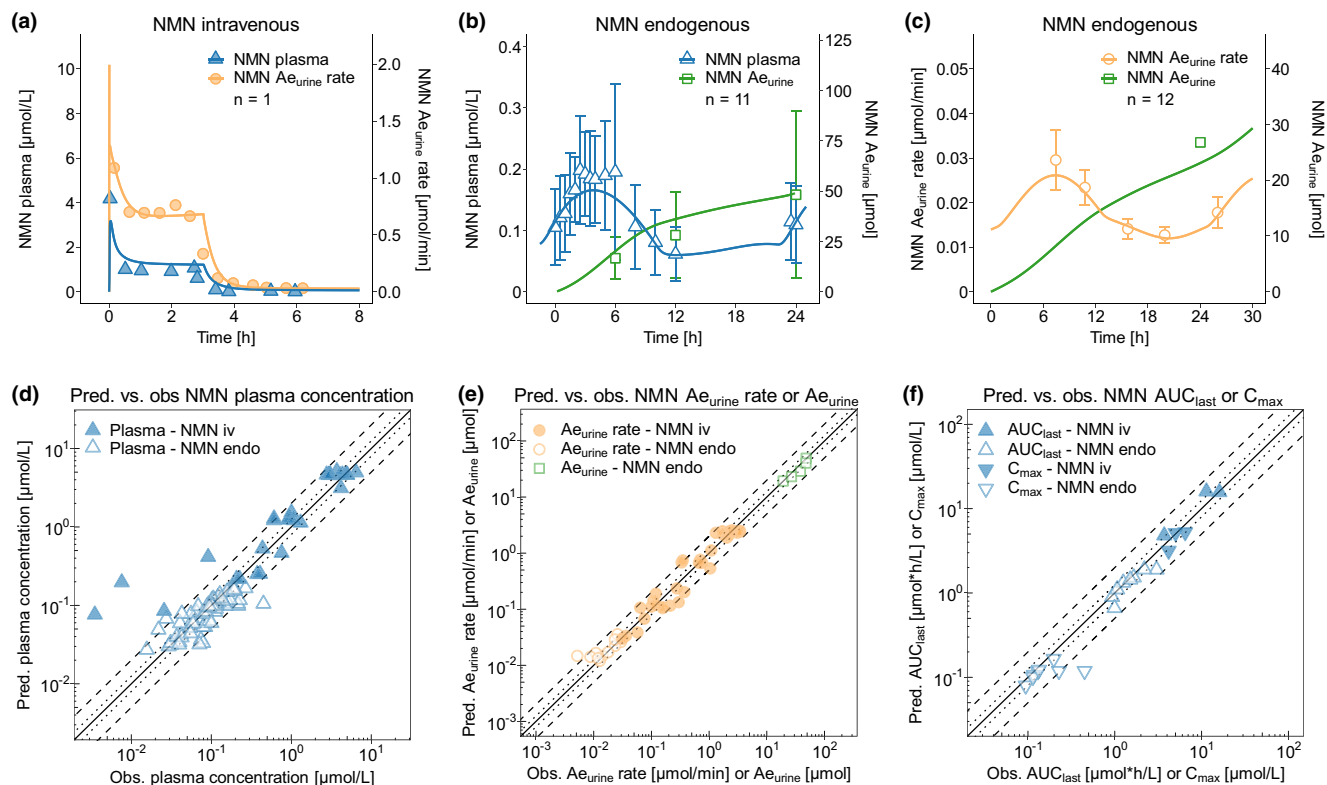


**Figure 4**  $N^1$ -methylnicotinamide (NMN) physiologically-based pharmacokinetic (PBPK) model performance. Predictions of NMN (a–c) plasma concentration–time (blue), urinary excretion rate ( $Ae_{urine}$  rate, orange), and cumulative amount excreted unchanged in urine ( $Ae_{urine}$ , green) profiles compared with observed data of representative studies<sup>7,9,10</sup> of a intravenous NMN administration of 8.3 mg loading dose followed by a 30.9 mg 3-hour infusion or b and c endogenous measurements. Time refers to the time after dose (exogenous) or time after first concentration measurement (endogenous). Goodness-of-fit plots showing predicted compared with observed NMN (d) plasma concentration, (e)  $Ae_{urine}$  and  $Ae_{urine}$  rate, and (f) area under the concentration–time curve ( $AUC_{last}$ ) and maximum plasma concentration ( $C_{max}$ ) values of all studies used for model building and evaluation. The solid line marks the line of identity and dotted lines indicate 1.25-fold and dashed lines indicate 2-fold deviation. Data are shown as blue triangles (plasma), orange dots ( $Ae_{urine}$  rate), and green squares ( $Ae_{urine}$ ); filled symbols indicate NMN administration, and empty symbols indicate endogenous NMN. Details on the clinical studies and individual values alongside mean relative deviations (MRDs) and geometric mean fold errors (GMFEs) are provided in **Supplementary Section S3**. Endo, endogenous; iv, intravenous;  $n$ , number of individuals studied; obs., observed; pred. predicted. [Colour figure can be viewed at [wileyonlinelibrary.com](https://onlinelibrary.wiley.com)]

also an apparently decreased diurnal variation. The mechanisms underlying these observations have not been described. Thus, it was hypothesized that trimethoprim and pyrimethamine inhibit nicotinamide N-methyltransferase (NNMT), and, hence, NMN synthesis. Consequently, an additional inhibition process of NMN  $R_{syn}$  was implemented (equation provided in **Supplementary Section S1.3**). After applying this hypothetical NNMT inhibition using optimized values for the inhibitory constant of NMN synthesis ( $K_{i,syn}$ ), with  $K_{i,syn} = 32.61 \mu\text{mol/L}$  and  $K_{i,syn} = 1.39 \mu\text{mol/L}$  for trimethoprim and pyrimethamine, respectively, in addition to inhibition of OCT2 and MATE1, urine and plasma-concentration–time profiles were well described, indicating a good drug–NMN interaction model performance. Representative predicted NMN profiles without and with inhibitor compared with observed data are shown in **Figure 7**. Plots of profiles are provided in **Supplementary Section S8**.

Predicted DBI  $AUC_{last}$ ,  $C_{max}$ , and  $Ae_{urine}$  ratios are all within twofold of observed ratios and within prediction limits proposed by Guest *et al.*<sup>34</sup> (**Figure 7**). Corresponding values for all clinical studies are provided in **Tables S43, S44, S45, S47, S48, and S49**, including calculated overall GMFEs.

## DISCUSSION

Whole-body PBPK models of the endogenous OCT2 and MATE1 substrates creatinine and NMN were built and thoroughly evaluated, accurately simulating and predicting plasma as well as urine profiles of both compounds. Two important scenarios were evaluated: (1) simulation and prediction of endogenous baseline creatinine and NMN as well as (2) creatinine and NMN kinetics after exogenous intake and administration. For this, PBPK models implemented relevant metabolism and transport processes and covered the influence of diurnal rhythm on significant physiological processes. These models have been successfully applied to simulate and predict the fate of creatinine and NMN during administration of trimethoprim, pyrimethamine, and cimetidine, focusing on renal transporter inhibition.

Since creatinine concentrations are not only affected by (co-)administered drugs, but also by important covariates, such as sex, age, body and muscle mass, diet, and disease state,<sup>36</sup> a holistic pharmacokinetic modeling approach is required to incorporate these factors. In lieu of previously published creatinine PBPK models that only focused on a specific topic (e.g., prediction of creatinine transporter interactions<sup>20–23</sup> or creatinine in chronic kidney disease<sup>37</sup>), the

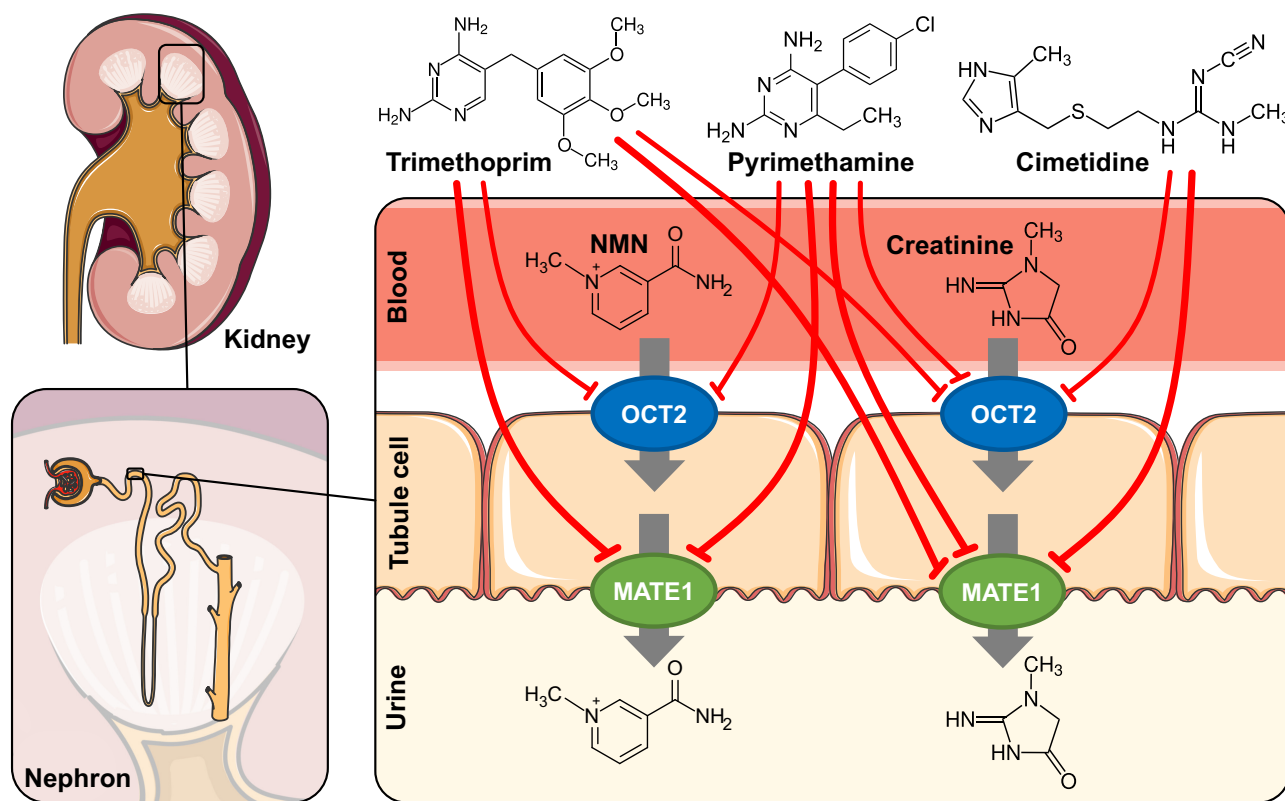


**Figure 5** Renal transporter drug-biomarker interaction network. Creatinine and N<sup>1</sup>-methylnicotinamide (NMN) are actively secreted into urine by sequential action of organic cation transporter (OCT)2, an influx transporter located at the basolateral membrane of proximal tubule epithelial cells, and multidrug and toxin extrusion protein (MATE)1, an efflux transporter located at the apical site of the same cells. Trimethoprim, pyrimethamine, and cimetidine are competitive inhibitors of OCT2 and MATE1, resulting in decreased renal excretion of creatinine and NMN. Gray arrows represent active transport, and red lines indicate transporter inhibition. Drawings by Servier, licensed under CC BY 3.0.<sup>44</sup> [Colour figure can be viewed at [wileyonlinelibrary.com](https://onlinelibrary.wiley.com/doi/10.1002/cpt.2636)]

presented whole-body PBPK model is the first to mechanistically describe creatinine synthesis in muscle cells with respect to varying muscle mass while incorporating diurnal renal elimination as well as renal transporter-mediated DBIs. Optimized values for creatinine synthesis in muscle cells exhibit a large intra- and interstudy variability, which is plausible due to the influence of the aforementioned covariates. Moreover, the effect of a creatinine-rich diet on plasma levels and urinary excretion is covered by the model, allowing simulation of creatinine kinetics after ingestion of differently prepared meat meals. Creatinine intake was implemented as an oral solution by calculating the ingested amount from the meal-specific creatinine content informed by the literature.<sup>29</sup> For this, creatinine must be absorbed from the gastrointestinal tract. Due to its hydrophilic properties, creatinine has been discussed as organic cation and anion transporter substrate,<sup>6</sup> which might also be relevant for the intestinal barrier. A significant increase in intestinal permeability has been observed after fitting simulations regarding oral creatinine intake in comparison to quantitative structure-activity relationship estimated permeability and might hint toward additional unspecified transport processes in the gut. At the renal barrier, organic anion transporter (OAT)2, OCT2, MATE1, and MATE2-K have been shown to transport creatinine *in vitro*<sup>6</sup> with OAT2 also discussed to be involved in creatinine re-absorption.<sup>38</sup> However, only tubular secretion via OCT2 and MATE1 has been

implemented in the model, as they show the most pronounced creatinine uptake *in vitro*.<sup>6</sup> Furthermore, a distinction between two transporters at the same membrane (i.e., OAT2 and OCT2), is challenging without knowledge of the amount transported and MATE2-K expression is controversial, as in a recent study, MATE2-K was below the lower limit of quantification in human kidneys.<sup>39</sup>

For the transporter substrate metformin, which is exclusively renally excreted, about 75% of clearance can be attributed to active secretion,<sup>2</sup> and diurnal variation of GFR, renal blood flow, and OCT2 activity have been observed to affect metformin pharmacokinetics (D. Türk *et al.*, unpublished data). As the same renal excretion axis is also relevant for creatinine, insights from metformin were transferred to the biomarker model. For creatinine, diurnal variation observed in plasma can be fully explained by varying GFR and renal blood flow, whereas only a neglectable amount can be attributed to varying OCT2 activity. This is in accordance with literature, as a much smaller extent of creatinine is actively secreted compared with metformin.<sup>2</sup> Fluctuation in creatinine synthesis attributed to varying activity of creatine kinase (e.g., due to physical activity<sup>40</sup>) might contribute to observed intraday variation in plasma concentrations and modeled diurnal synthesis showed expected plasma level pattern. However, varying GFR and renal blood flow already lead to an adequate description of observed data with parametrization derived

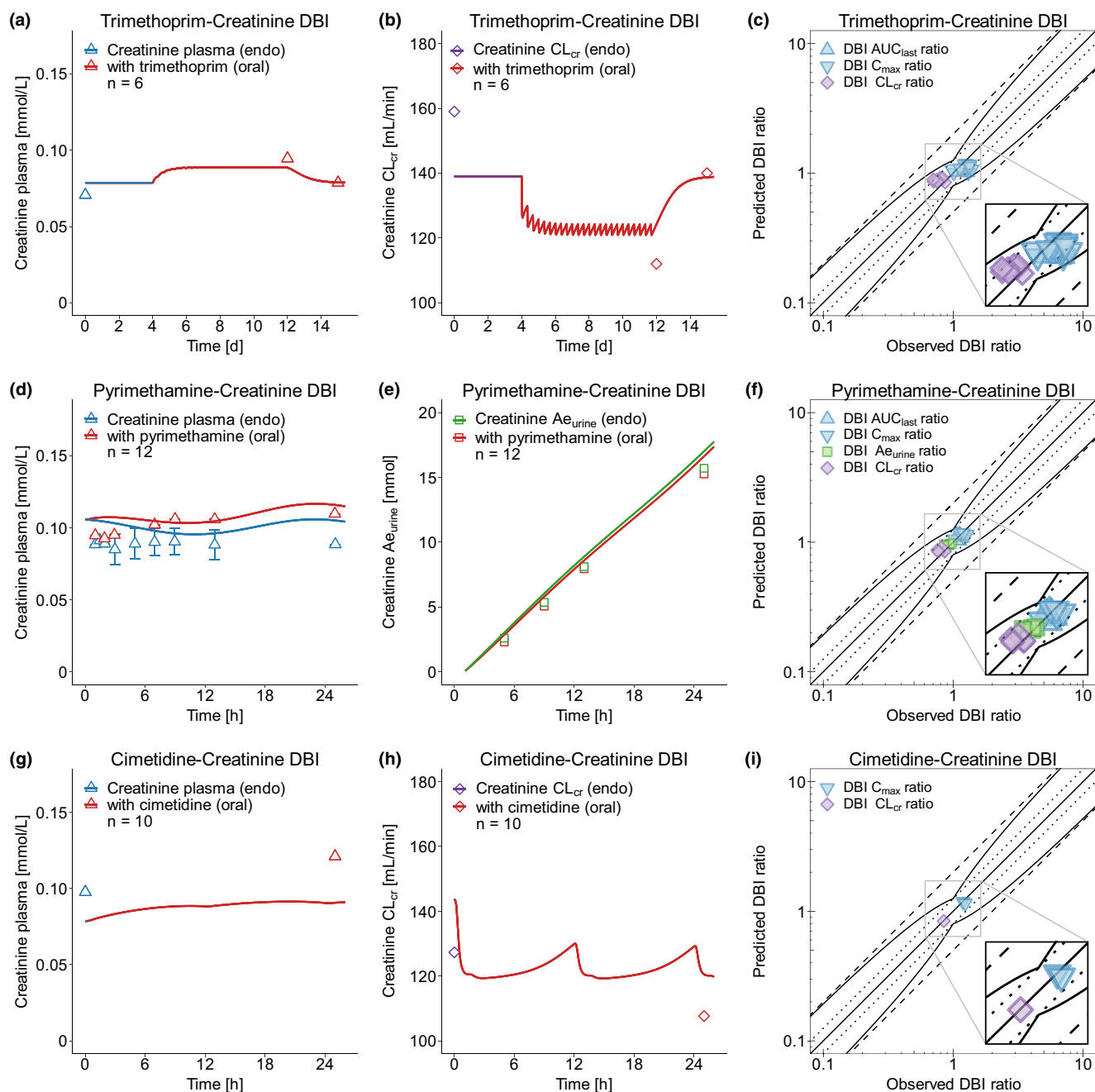


**Figure 6** Drug-creatinine interaction model performance. Predictions of creatinine plasma concentration-time (blue), renal creatinine clearance ( $CL_{cr}$ , purple), and cumulative amount excreted unchanged in urine ( $Ae_{urine}$ , green) profiles of the (a, b) trimethoprim-creatinine, (d, e) pyrimethamine-creatinine, and (g, h) cimetidine-creatinine interactions, compared with observed data.<sup>35,48,49</sup> Predictions are shown as lines. Predicted compared with observed DBI area under the concentration-time curve ( $AUC_{last}$ ), maximum plasma concentration ( $C_{max}$ ),  $Ae_{urine}$ , and  $CL_{cr}$  ratios of all clinical studies used are shown to evaluate the performance of the (c) trimethoprim-creatinine, (f) pyrimethamine-creatinine, and (i) cimetidine-creatinine interaction models. The straight solid line marks the line of identity and the curved solid lines show the DBI prediction acceptance limits proposed by Guest *et al.*<sup>34</sup> Dotted lines indicate 1.25-fold and dashed lines indicate 2-fold deviation. Data are shown as blue triangles (DBI  $AUC_{last}$  and  $C_{max}$  ratios), green squares (DBI  $Ae_{urine}$  ratios) or purple diamonds (DBI  $CL_{cr}$  ratios). Details on the study protocols, model simulations and individual DBI  $AUC_{last}$ ,  $C_{max}$ ,  $Ae_{urine}$ , and  $CL_{cr}$  ratios of all clinical studies used to evaluate the DBI performance of the creatinine model are provided in **Supplementary Section S7**. DBI, drug-biomarker interaction; endo, endogenous; n, number of individuals studied. [Colour figure can be viewed at [wileyonlinelibrary.com](http://wileyonlinelibrary.com)]

from previously reported values. Therefore, diurnal synthesis has not been implemented in the final model.

The implementation of only two renal transporters for tubular secretion might limit the creatinine model regarding physiological

precision, which could be overcome by further research in this area, especially regarding transporters involved in re-absorption. Moreover, the number of well-controlled creatinine studies, especially with nonaggregated data, is limited and many older studies,



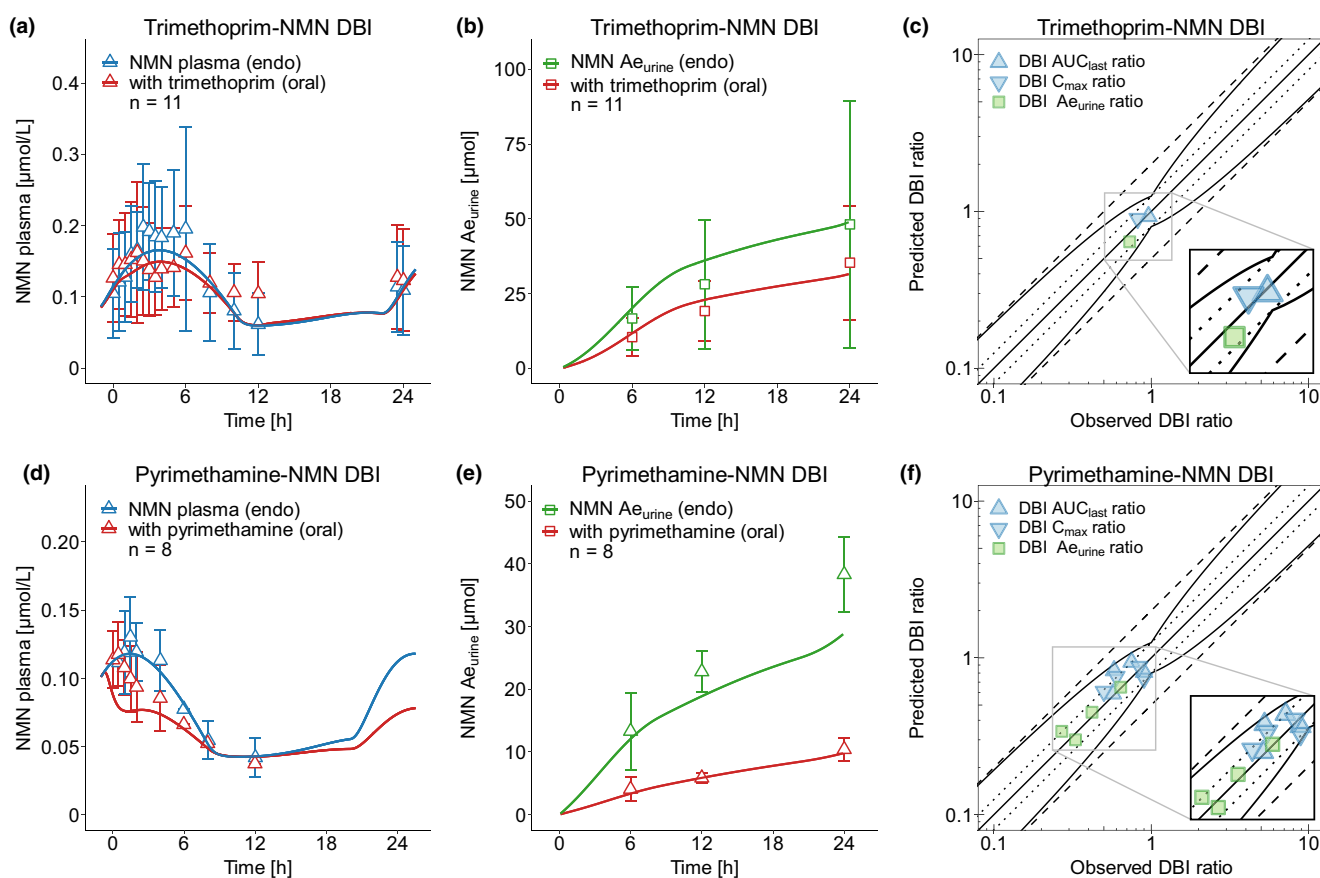


**Figure 7** Drug- $N^1$ -methylnicotinamide (NMN) interaction model performance. Predictions of NMN plasma concentration-time (blue) and cumulative amount excreted unchanged in urine ( $Ae_{urine}$ , green) profiles of the (a, b) trimethoprim-NMN and (d, e) pyrimethamine-NMN interactions, compared with observed data.<sup>8,9</sup> Predictions are shown as lines. Predicted compared with observed DBI area under the concentration-time curve ( $AUC_{last}$ ), maximum plasma concentration ( $C_{max}$ ), and  $Ae_{urine}$  ratios of all clinical studies used are shown to evaluate the performance of the (c) trimethoprim-NMN and (f) pyrimethamine-NMN interaction models. The straight solid line marks the line of identity and the curved solid lines show the DBI prediction acceptance limits proposed by Guest *et al.*<sup>34</sup> Dotted lines indicate 1.25-fold and dashed lines indicate 2-fold deviation. Data are shown as blue triangles (DBI  $AUC_{last}$  and  $C_{max}$  ratios) or green squares (DBI  $Ae_{urine}$  ratios). Details on the study protocols, model simulations and individual DBI  $AUC_{last}$ ,  $C_{max}$ , and  $Ae_{urine}$  ratios of all clinical studies used to evaluate the DBI performance of the NMN model are provided in **Supplementary Section S8**. DBI, drug-biomarker interaction; endo, endogenous;  $n$ , number of individuals studied. [Colour figure can be viewed at [wileyonlinelibrary.com](http://wileyonlinelibrary.com)]

used in model development and evaluation, measured creatinine by varying analytical methods which might contribute to inter-study variability of creatinine levels that are already prone to large inter- and intraindividual differences, including diurnal variation. Nevertheless, the final model met the required model performance evaluation criteria, typically applied to drug models<sup>17,25</sup> and all predicted plasma and urine concentrations deviated less than twofold from the observed data.

The NMN PBPK model presented in this work is the first kinetic model of this biomarker, mechanistically describing its synthesis, biotransformation, tubular secretion, and re-absorption. Because no NMN  $R_{syn}$  has been reported yet, an approximate value for NMN  $R_{syn}$  has been calculated from measurements of NMN and its carboxamide metabolites in urine,<sup>7</sup> assuming no further metabolization. This revealed an NMN  $R_{syn}$  of about 77  $\mu\text{mol}$  per day, which is much lower than the creatinine synthesis of about 18 mmol per day.<sup>41</sup>

NMN is metabolized by AOX1 and urinary excretion rates of NMN and its metabolites in urine were also utilized to assess the fraction of endogenous NMN metabolized, revealing that about

65% of NMN undergo further biotransformation.<sup>7</sup> Regarding renal excretion, a saturable tubular re-absorption process has been described in addition to tubular secretion via OCT2 and MATEs, as the ratio of renal NMN clearance and creatinine clearance is concentration dependent.<sup>10</sup> A transport process has been implemented at the basolateral site of tubule epithelial cells, informing Michaelis-Menten and transport rate constant values by simultaneously fitting observed plasma and urine data to simulations of endogenous NMN and after intravenous administration, leading to an accurate description of NMN levels. However, involved transporters, their location in the kidneys, the mechanism of transportation, and real NMN concentrations in kidney cells remain unknown. Moreover, sequential actions of two transporters are also plausible, which requires further investigations.

In contrast to modeling metformin (D. Türk *et al.*, unpublished data) and creatinine, the pronounced diurnal variation in observed NMN plasma concentrations could not be sufficiently described by solely implementing a diurnal rhythm of GFR, renal blood flow, and OCT2, as each of these accounted for only 0%, 1%, and 9% of

the observed amplitude, respectively. This variation could be explained, however, by the large influence of varying synthesis due to nicotinamide adenine dinucleotide utilization and, hence, affected nicotinamide levels.<sup>7</sup> Therefore, a mixed effect of diurnal synthesis and elimination was assumed to model NMN in plasma and urine. For this, the model implements an additional intermittent synthesis process with study-specific optimized values for amplitude and acrophase to address the observed large interstudy variability (Table S13). These differences might be attributed to expected intersubject variability in activity levels before the first NMN measurement that are correlated to NAD utilization. Additionally, a diurnal pattern of AOX4 activity has been observed in Harderian glands of mice,<sup>42</sup> but was not considered in the model, as data in humans are lacking and effect separation (e.g., from diurnal elimination) is not possible analyzing the available clinical data on urine measurements of NMN carboxamide metabolites.

Due to lack of information and data, some assumptions have been made during the development of the NMN model. This included uninformed priors regarding the extent of synthesis and involved transporters at the renal barrier as well as the diurnal processes to cover highly variable intraday NMN plasma levels. Moreover, the large observed interindividual differences in NMN plasma levels have been modeled by implementing a varying extent of NMN synthesis. However, only a limited number of studies could be included during model development, because many studies reported only very sparse NMN plasma data without specification of clock time. Furthermore, only studies on healthy subjects could be included, as increased expression of NNMT has been described (e.g., in patients with cancer, metabolic, and cardiovascular diseases<sup>43</sup>), where NMN levels should be interpreted with great caution. Despite these challenges, the PBPK model met the performance evaluation criteria with about 90% of predicted plasma and urine concentrations within twofold of observed data.

Sensitivity analyses of both biomarkers reveal highest sensitivity to the fraction unbound in plasma, where a literature value of 100% was used in both models. Furthermore, the analyses highlight the most important model processes, showing that transporter-mediated tubular secretion plays a minor role for creatinine pharmacokinetics compared with NMN.

This work was complemented by the development and evaluation of a DDI/DBI network involving three perpetrators of OCT2 and MATE1, trimethoprim, pyrimethamine, and cimetidine, all previously evaluated for DDI predictions with metformin, and extended by models of the endogenous substrates, creatinine and NMN. According to the magnitude of  $K_i$  values and simulated (unbound) plasma and kidney concentrations, the main contributor to DDIs/DBIs is MATE inhibition. Whereas interactions lead to an expected decrease in renal clearance and increase in plasma levels of creatinine, similar interaction scenarios lead to a decrease in NMN renal clearance with simultaneously paradox decrease in plasma levels. Previously, this effect has been attributed to a possible inhibition of NMN synthesis by trimethoprim and pyrimethamine with unclear underlying mechanisms.<sup>1</sup> Hence, recent recommendations suggest focusing on NMN renal clearance instead of plasma concentrations during renal transporter perpetrator drug administration.<sup>1,8,11</sup> To apply PBPK models for

transporter-mediated interaction predictions, a close interdisciplinary collaboration between pharmacometricians and laboratory scientists should be enforced, to obtain reliable  $K_i$  values.

Because PBPK modeling is helpful for hypothesis generation and testing, inhibition of NMN synthesis by trimethoprim and pyrimethamine was implemented, leading to a satisfactory description of observed data by including  $K_i$  values at the same scale as OCT2 inhibition. Underlying effects, such as direct inhibition of NNMT, indirect NNMT inhibition due to reduction of the methyl donor S-adenosylmethionine by interference with human folate metabolism (trimethoprim and pyrimethamine are both inhibitors of bacterial folate metabolism), or direct interaction with the methionine cycle might be plausible. To verify or reject these hypotheses, additional *in vitro* inhibition assays and, especially, *in vivo* metabolomic investigations are necessary.

The previously mentioned covariates, such as muscle mass and disease state, might compromise the suitability of creatinine as a biomarker to assess transporter-mediated DDIs. However, the new creatinine PBPK model can compensate for these shortcomings. Standardized measurements of this low-cost and easily detectable marker supported by model-based analyses in early drug development will allow to gain insights into possible transporter-mediated interactions. NMN has been previously proposed to be a more suitable biomarker, due to the higher proportion of active secretion compared with creatinine (70% vs. 10–40%<sup>2,5</sup>) and good correlation of NMN and metformin renal clearances,<sup>35</sup> also applying to the trimethoprim-induced reduction of renal clearances.<sup>9</sup> The newly developed NMN PBPK model can support NMN measurements in context of a biomarker-informed strategy during drug development, as changes in NMN urine as well as plasma during interactions can be assessed and further strengthens the validity of the whole interaction network of three perpetrators and three victims.

In summary, whole-body PBPK models of the currently proposed biomarkers for OCT2 and MATE1 activity, creatinine, and NMN, have been developed that support the vision of a biomarker-informed strategy to improve DDI investigations during drug development. Here, all perpetrator and victim models were thoroughly studied and validated in a comprehensive interaction network. During development and evaluation stages, knowledge gaps could be identified as starting point for future research. The comprehensive models can be further extended (e.g., to include predictions in renally impaired individuals) and will be shared with the research and drug development community ([www.open-systems-pharmacology.org](http://www.open-systems-pharmacology.org)), to assist in future OCT2 and MATE interaction studies. Next to depicting a complement to a proposed biomarker-informed workflow,<sup>2</sup> a further biomarker model application might be the estimation of *in vivo*  $K_i$  values from phase I biomarker measurements without prior knowledge of interaction potential from *in vitro* tests.

#### SUPPORTING INFORMATION

Supplementary information accompanies this paper on the *Clinical Pharmacology & Therapeutics* website ([www.cpt-journal.com](http://www.cpt-journal.com)).

#### FUNDING

This project was partly funded by the German Federal Ministry of Education and Research (BMBF), grant number 031L0161C (“OSMOSES”). Open Access funding enabled and organized by Projekt DEAL.

**CONFLICT OF INTEREST**

F.M. is an employee of Boehringer Ingelheim Pharma GmbH & Co. KG. All other authors declared no competing interests for this work.

**AUTHOR CONTRIBUTIONS**

D.T., F.M., M.F.F., D.S., R.D., and T.L. wrote the manuscript. D.T. and T.L. designed the research. D.T. performed the research. D.T., F.M., M.F.F., D.S., R.D., and T.L. analyzed the data.

© 2022 The Authors. *Clinical Pharmacology & Therapeutics* published by Wiley Periodicals LLC on behalf of American Society for Clinical Pharmacology and Therapeutics.

This is an open access article under the terms of the [Creative Commons Attribution-NonCommercial](https://creativecommons.org/licenses/by-nc/4.0/) License, which permits use, distribution and reproduction in any medium, provided the original work is properly cited and is not used for commercial purposes.

- Shen, H. A pharmaceutical industry perspective on transporter and CYP-mediated drug-drug interactions: kidney transporter biomarkers. *Bioanalysis* **10**, 625–631 (2018).
- Mathialagan, S., Feng, B., Rodrigues, A.D. & Varma, M.V.S. Drug-drug interactions involving renal OCT2/MATE transporters: clinical risk assessment may require endogenous biomarker-informed approach. *Clin. Pharmacol. Ther.* **110**, 855–859 (2021).
- Oswald, S. *et al.* Protein abundance of clinically relevant drug transporters in the human kidneys. *Int. J. Mol. Sci.* **20**, 1–12 (2019).
- Fromm, M.F. Prediction of transporter-mediated drug-drug interactions using endogenous compounds. *Clin. Pharmacol. Ther.* **92**, 546–548 (2012).
- Levey, A.S., Perrone, R.D. & Madias, N.E. Serum creatinine and renal function. *Ann. Rev. Med.* **39**, 465–490 (1988).
- Mathialagan, S., Rodrigues, A.D. & Feng, B. Evaluation of renal transporter inhibition using creatinine as a substrate in vitro to assess the clinical risk of elevated serum creatinine. *J. Pharm. Sci.* **106**, 2535–2541 (2017).
- Okamoto, H. *et al.* Diurnal variations in human urinary excretion of nicotinamide catabolites: effects of stress on the metabolism of nicotinamide. *Am. J. Clin. Nutr.* **77**, 406–410 (2003).
- Ito, S. *et al.* N-methylnicotinamide is an endogenous probe for evaluation of drug-drug interactions involving multidrug and toxin extrusions (MATE1 and MATE2-K). *Clin. Pharmacol. Ther.* **92**, 635–641 (2012).
- Müller, F. *et al.* N(1)-methylnicotinamide as an endogenous probe for drug interactions by renal cation transporters: studies on the metformin-trimethoprim interaction. *Eur. J. Clin. Pharmacol.* **71**, 85–94 (2015).
- Weber, W., Toussaint, S., Looby, M., Nitz, M. & Kewitz, H. System analysis in multiple dose kinetics: evidence for saturable tubular reabsorption of the organic cation N1-methylnicotinamide in humans. *J. Pharmacokinetic. Biopharm.* **19**, 553–574 (1991).
- Müller, F., Sharma, A., König, J. & Fromm, M.F. Biomarkers for in vivo assessment of transporter function. *Pharmacol. Rev.* **70**, 246–277 (2018).
- Rodrigues, A.D., Taskar, K.S., Kusuvara, H. & Sugiyama, Y. Endogenous probes for drug transporters: balancing vision with reality. *Clin. Pharmacol. Ther.* **103**, 434–448 (2018).
- Chu, X. *et al.* Clinical probes and endogenous biomarkers as substrates for transporter drug-drug interaction evaluation: perspectives from the International Transporter Consortium. *Clin. Pharmacol. Ther.* **104**, 836–864 (2018).
- Grimstein, M. *et al.* Physiologically based pharmacokinetic modeling in regulatory science: an update from the U.S. Food and Drug Administration's Office of Clinical Pharmacology. *J. Pharm. Sci.* **108**, 21–25 (2019).
- Türk, D. *et al.* Physiologically based pharmacokinetic models for prediction of complex CYP2C8 and OATP1B1 (SLC01B1) drug-drug-gene interactions: a modeling network of gemfibrozil, repaglinide, pioglitazone, rifampicin, clarithromycin and itraconazole. *Clin. Pharmacokinetic.* **58**, 1595–1607 (2019).
- Türk, D. *et al.* Novel models for the prediction of drug-gene interactions. *Expert Opin. Drug Metab. Toxicol.* **17**, 1293–1310 (2021).
- Hanke, N. *et al.* A comprehensive whole-body physiologically based pharmacokinetic drug–drug–gene interaction model of metformin and cimetidine in healthy adults and renally impaired individuals. *Clin. Pharmacokinetic.* **59**, 1419–1431 (2020).
- Yoshikado, T. *et al.* PBPK modeling of coproporphyrin I as an endogenous biomarker for drug interactions involving inhibition of hepatic OATP1B1 and OATP1B3. *CPT Pharmacometrics Syst. Pharmacol.* **7**, 739–747 (2018).
- Takita, H. *et al.* PBPK model of coproporphyrin I: evaluation of the impact of SLC01B1 genotype, ethnicity, and sex on its inter-individual variability. *CPT Pharmacometrics Syst. Pharmacol.* **10**, 137–147 (2021).
- Nakada, T., Kudo, T., Kume, T., Kusuvara, H. & Ito, K. Quantitative analysis of elevation of serum creatinine via renal transporter inhibition by trimethoprim in healthy subjects using physiologically-based pharmacokinetic model. *Drug Metab. Pharmacokinetic.* **33**, 103–110 (2018).
- Nakada, T., Kudo, T., Kume, T., Kusuvara, H. & Ito, K. Estimation of changes in serum creatinine and creatinine clearance caused by renal transporter inhibition in healthy subjects. *Drug Metab. Pharmacokinetic.* **34**, 233–238 (2019).
- Imamura, Y. *et al.* Prediction of fluoroquinolone-induced elevation in serum creatinine levels: a case of drug-endogenous substance interaction involving the inhibition of renal secretion. *Clin. Pharmacol. Ther.* **89**, 81–88 (2011).
- Scotcher, D. *et al.* Mechanistic models as framework for understanding biomarker disposition: prediction of creatinine-drug interactions. *CPT Pharmacometrics Syst. Pharmacol.* **9**, 282–293 (2020).
- U.S. Food and Drug Administration. *Drug development and drug interactions: table of substrates, inhibitors and inducers.* <<https://www.fda.gov/drugs/drug-interactions-labeling/drug-development-and-drug-interactions-table-substrates-inhibitors-and-inducers>> (2017). Accessed March 1, 2022.
- Türk, D., Hanke, N. & Lehr, T. A physiologically-based pharmacokinetic model of trimethoprim for MATE1, OCT1, OCT2, and CYP2C8 drug-drug-gene interaction predictions. *Pharmaceutics* **12**, 1074 (2020).
- Sjögren, E., Tarning, J., Barnes, K.I. & Jonsson, E.N. A physiologically-based pharmacokinetic framework for prediction of drug exposure in malnourished children. *Pharmaceutics* **13**, 204 (2021).
- Mitchell, M., Muftakhidinov, B. & Winchen, T. *Engauge Digitizer Software.* <<https://markummitchell.github.io/engauge-digitizer>>. Accessed March 1, 2022.
- Wojtyniak, J.-G., Britz, H., Selzer, D., Schwab, M. & Lehr, T. Data digitizing: accurate and precise data extraction for quantitative systems pharmacology and physiologically-based pharmacokinetic modeling. *CPT Pharmacometrics Syst. Pharmacol.* **9**, 322–331 (2020).
- Camara, A.A., Arn, K.D., Reimer, A. & Newburgh, L.H. The twenty-four hourly endogenous creatinine clearance as a clinical measure of the functional state of the kidneys. *J. Lab. Clin. Med.* **37**, 743–763 (1951).
- Jacobsen, F.K., Christensen, C.K., Mogensen, C.E., Andreasen, F. & Heilskov, N.S. Postprandial serum creatinine increase in normal subjects after eating cooked meat. *Proc. Eur. Dial. Transpl. Assoc.* **16**, 506–512 (1979).
- Mayersohn, M., Conrad, K.A. & Achari, R. The influence of a cooked meat meal on creatinine plasma concentration and creatinine clearance. *Br. J. Clin. Pharmacol.* **15**, 227–230 (1983).
- Perlzweig, W.A. & Huff, J.W. The fate of N1-methylnicotinamide in man. *J. Biol. Chem.* **161**, 417 (1945).
- Lehr, T. *et al.* A quantitative enterohepatic circulation model. *Clin. Pharmacokinetic.* **48**, 529–542 (2009).
- Guest, E.J., Aarons, L., Houston, J.B., Rostami-Hodjegan, A. & Galetin, A. Critique of the two-fold measure of prediction success for ratios: application for the assessment of drug-drug interactions. *Drug Metab. Dispos.* **39**, 170–173 (2011).
- Miyake, T. *et al.* Identification of appropriate endogenous biomarker for risk assessment of multidrug and toxin extrusion

- protein-mediated drug-drug interactions in healthy volunteers. *Clin. Pharmacol. Ther.* **109**, 507–516 (2021).
36. Chu, X., Chan, G.H. & Evers, R. Identification of endogenous biomarkers to predict the propensity of drug candidates to cause hepatic or renal transporter-mediated drug-drug interactions. *J. Pharm. Sci.* **106**, 2357–2367 (2017).
37. Takita, H., Scotcher, D., Chinnadurai, R., Kalra, P.A. & Galetin, A. Physiologically-based pharmacokinetic modelling of creatinine-drug interactions in the chronic kidney disease population. *CPT Pharmacometrics Syst. Pharmacol.* **9**, 695–706 (2020).
38. Chu, X., Bleasby, K., Chan, G.H., Nunes, I. & Evers, R. The complexities of interpreting reversible elevated serum creatinine levels in drug development: Does a correlation with inhibition of renal transporters exist? *Drug Metab. Dispos.* **44**, 1498–1509 (2016).
39. Prasad, B. *et al.* Abundance of drug transporters in the human kidney cortex as quantified by quantitative targeted proteomics. *Drug Metab. Dispos.* **44**, 1920–1924 (2016).
40. Gutenbrunner, C. Circadian variations of the serum creatine kinase level—a masking effect? *Chronobiol. Int.* **17**, 583–590 (2000).
41. Feher, J. (ed.) 7.4—Tubular reabsorption and secretion. In *Quantitative Human Physiology* 719–729 (Academic Press, Boston, 2017).
42. Terao, M. *et al.* Mouse aldehyde-oxidase-4 controls diurnal rhythms, fat deposition and locomotor activity. *Sci. Rep.* **6**, 30343 (2016).
43. Gao, Y. *et al.* Bisubstrate inhibitors of nicotinamide N-methyltransferase (NNMT) with enhanced activity. *J. Med. Chem.* **62**, 6597–6614 (2019).
44. Les Laboratoires Servier. *Servier Medical Art.* <<https://smart.servier.com/>>. Accessed November 30, 2021.
45. Berglund, F., Killander, J. & Pompeius, R. Effect of trimethoprim-sulfamethoxazole on the renal excretion of creatinine in man. *J. Urol.* **114**, 802–808 (1975).
46. Pasternack, A. & Kuhlback, B. Diurnal variations of serum and urine creatine and creatinine. *Scand. J. Clin. Lab. Invest.* **27**, 1–7 (1971).
47. Pissios, P. Nicotinamide N-methyltransferase: more than a vitamin B3 clearance enzyme. *Trends Endocrinol. Metab.* **28**, 340–353 (2017).
48. Shouval, D., Ligumsky, M. & Ben-Ishay, D. Effect of co-trimoxazole on normal creatinine clearance. *Lancet* **1**, 244–245 (1978).
49. Serdar, M.A. *et al.* A practical approach to glomerular filtration rate measurements: creatinine clearance estimation using cimetidine. *Ann. Clin. Lab. Sci.* **31**, 265–273 (2001).